Laser and Particle Beams (2003), *21*, 7–11. Printed in the USA.

DOI: 10.1017/S0263034602211027

Stopping power of dense helium plasma for fast heavy ions

J. HASEGAWA,[1] N. YOKOYA,[1] Y. KOBAYASHI,[1] M. YOSHIDA,[1] M. KOJIMA,[1] T. SASAKI,[1] H. FUKUDA,[1] M. OGAWA,[1] Y. OGURI,[1] AND T. MURAKAMI[2]

[1]Research Laboratory for Nuclear Reactors, Tokyo Institute of Technology, Tokyo, Japan
[2]National Institute of Radiological Sciences, Chiba-shi, Japan

(RECEIVED 27 May 2002; ACCEPTED 20 June 2002)

Abstract

The interaction process between fast heavy ions and dense plasma was experimentally investigated. We injected 4.3-MeV/u or 6.0-MeV/u iron ions into a *z*-pinch-discharge helium plasma and measured the energy loss of the ions by the time of flight method. The energy loss of 4.3-MeV/u ions fairly agreed with theoretical prediction when the electron density of the target was on the order of 10^{18} cm^{-3}. With increasing electron density beyond 10^{19} cm^{-3}, the difference between the experiment and the theory became remarkable; the experimental energy loss was 15% larger than the theoretical value at the peak density. For 6.0-MeV/u ions, the deviation from the theory appeared even at densities below 10^{19} cm^{-3}. These discrepancies indicated that density effects such as ladderlike ionization caused the enhancement of the projectile mean charge in the target.

Keywords: Beam–plasma interaction; Heavy ion fusion; Stopping power; *Z*-pinch plasma

1. INTRODUCTION

The stopping power of dense plasma for heavy ions is an important topic in heavy ion fusion research because it determines beam energy deposition in a fuel target. Beam–plasma interaction experiments have revealed the enhancement of the stopping power due to plasma effects (Young *et al.*, 1982; Hoffmann *et al.*, 1990; Couillaud *et al.*, 1994; Jacoby *et al.*, 1995). Most of the experiments used discharge plasma targets because they were superior in uniformity, line density, and lifetime to the other plasma targets such as laser-produced plasmas. However, the strong magnetic field induced by large discharge current often prevented the beams from penetrating the target effectively, which resulted in unwanted beam signal attenuation (plasma-lens effect). This trade-off between the beam signal and the discharge current has limited the plasma density to 10^{17}–10^{18} cm^{-3}. Although the capillary discharge has the potential to produce plasmas with an electron density over 10^{19} cm^{-3} under relatively low discharge current, the diagnostics is very difficult because of the complex plasma composition.

We have so far measured the energy loss of 6.0-MeV/u ions in a *z*-pinch helium plasma under electron densities on the order of 10^{18} cm^{-3} (Hasegawa *et al.*, 2001). To examine the beam interaction processes in denser plasmas, we optimized both the discharge conditions and the beam transport with the help of numerical calculations. As a result, we succeeded in increasing the plasma density and observing the energy loss of the ions even at lower injection energy. This report presents experimental results on the energy loss of 4.3-MeV/u or 6.0-MeV/u iron ions in a helium plasma with electron densities above 10^{19} cm^{-3}. We also discuss the dependence of the energy loss on the beam velocity and the plasma density.

2. EXPERIMENT

Figure 1 illustrates the experimental setup for measurement of the energy loss of heavy ions in a *z*-pinch plasma target. A 30-mm-inner-diameter quartz tube initially contained helium gas of 300 Pa. While charging a capacitor, a high-voltage power source also preionized the helium gas with glow discharge, which guaranteed the uniformity of the suc-

Address correspondence and reprint requests to: Jun Hasegawa, Research Laboratory for Nuclear Reactors, Tokyo Institute of Technology, 2-12-1, O-okayama, Meguro-ku, Tokyo, 152-8550, Japan. E-mail: jhasegaw@nr.titech.ac.jp

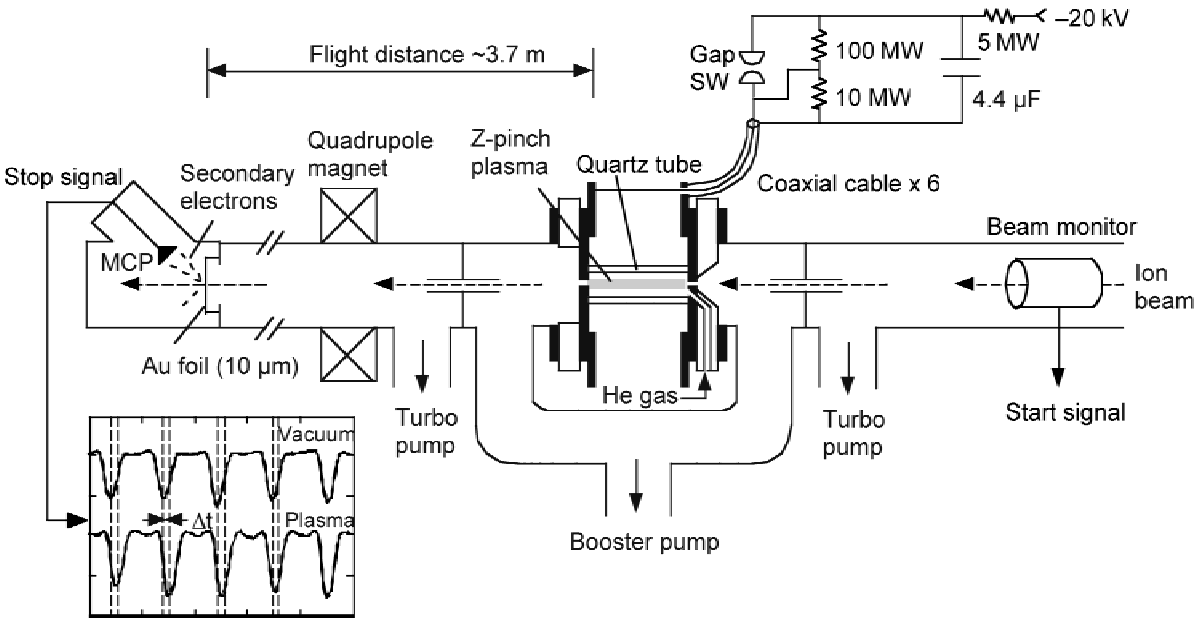

Fig. 1. An experimental setup for energy loss measurement using a *z*-pinch plasma target.

ceeding main discharge. The main discharge current had a sinusoidal waveform of 70 kA in amplitude and 4 μs in half period. A dense plasma column of about 16 cm long formed on the beam axis 1 μs after the discharge ignition.

We determined the electron density of the plasma target from the Stark broadening of He_{II} P_α line (468.6 nm) using an empirical scaling given by Büscher *et al.* (1996). The uncertainty of the scaling is about $\pm$10%. The electron temperature was determined from the line intensity ratio of He_{II} P_α and He_I 1*s*2*p*-1*s*3*d* (567.7 nm) under a LTE assumption (Griem, 1997). The time evolution of these two lines was simultaneously recorded using a combination of a spectroscope and a streak camera. By moving the observation point along the beam axis, we observed also the axial distributions of the plasma parameters.

For interaction experiments, we used ^{56}Fe beams with an injection energy of 4.3 MeV/u or 6.0 MeV/u supplied from RF linacs of HIMAC at the National Institute of Radiological Sciences. The projectile ions entered the target through a 1-mm-diameter aperture on the discharge anode and then interacted with the plasma column. After exiting from the target, the ions were focused by a quadrupole doublet onto a 10-μm-thick gold foil at 3.7 m downstream. A micro-channel-plate (MCP) assembly detected secondary electrons emerging from the foil and amplified the signals. From a delay in the arrival time of each beam bunch at the detector, we extracted the energy loss of the ions in the target.

3. NUMERICAL ANALYSIS

To support the plasma diagnostics, we also performed numerical calculations of a *z*-pinch plasma using a one-dimensional MHD simulation code (Aoki *et al.*, 1995). We did not consider the coupling between the plasma load and the external circuit because it had little influence on the current waveform in our circuit-parameter range. The simulation results were not only compared with the results of the plasma spectroscopy, but also used to optimize the beam transport from the plasma target to the MCP detector.

To give theoretical predictions we calculated the energy loss of the projectile using a stopping-power formula for partially ionized plasma (Peter & Meyer-ter-Vehn, 1991). The calculation solved rate equations to obtain the projectile mean charge in each time step, which self-consistently included the changes of ionization and recombination cross sections due to the decrease in projectile velocity. Here we considered the following atomic processes for ground levels: collisional ionization by plasma ions or free electrons, bound electron capture, and radiative electron capture.

4. RESULTS AND DISCUSSIONS

Figure 2 summarizes the results of both the plasma spectroscopy and the numerical analysis using a MHD code. The electron density and temperature reached 1.2×10^{19} cm^{-3} and 6.3 eV after about 1 μs from the ignition, which was almost consistent with the simulation results. The plasma target length was determined to be 15.5 cm from the axial profile of the electron density. Thus, the line density of the target exceeded 10^{20} cm^{-2}. The self-consistent solution of the Saha equations showed that the mean charge state of the plasma ions was 1.5 at the peak density.

Figure 3 plots the energy losses of 4.3-MeV/u and 6.0-MeV/u ^{56}Fe ions as a function of time. Thanks to beam transport optimization, we could observe the energy loss over the pinch process without serious beam signal attenu-

https://doi.org/10.1017/S0263034602211027 Published online by Cambridge University Press

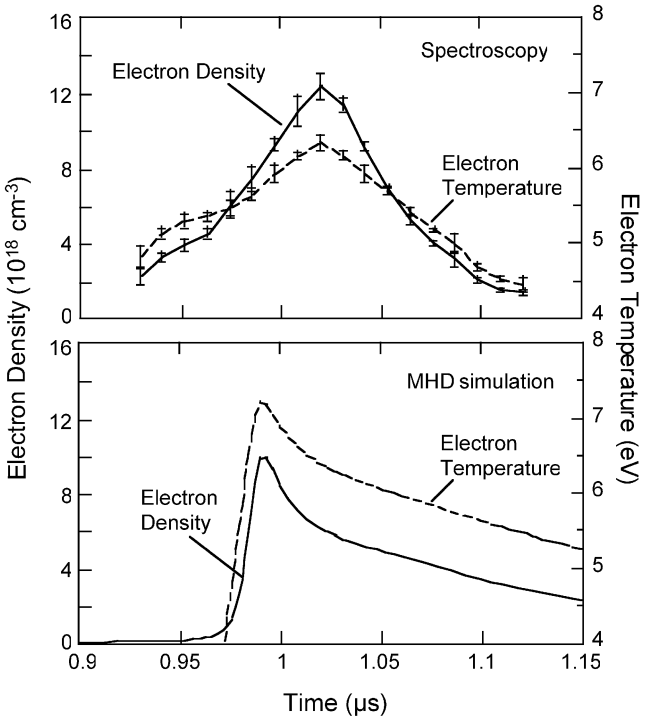

Fig. 2. Electron densities and electron temperatures of target plasma estimated by plasma spectroscopy and numerical analyses using a MHD code.

ation. Particularly at the peak density the observed energy losses were much larger than those in a cold equivalent from TRIM (29.8 MeV for 4.3 MeV/u ^{56}Fe, 25.3 MeV for 6.0 MeV/u ^{56}Fe). This large enhancement showed that although the plasma target was not fully ionized, plasma free electrons dominated the interaction processes. Note that the energy loss was almost independent of the initial charge of the projectile, meaning that the projectile experienced similar evolution of the mean charge. The calculation of the projectile mean charge also supported these results.

In Figure 4, we plot the energy loss of iron ions under a target electron density of 1.2×10^{19} cm^{-3} as a function of injection energy. The figure also shows theoretical energy-loss curves for Fe^{22+} injection (upper solid line) and Fe^{23+} injection (lower solid line); the difference between the curves is small enough to be neglected. We found that both experimental values largely exceeded the theoretical predictions by 15–20%.

The dependences of the energy loss of 4.3-MeV/u and 6.0-MeV/u ^{56}Fe ions on the target electron density are shown in Figure 5. Theoretical predictions of the energy loss are also plotted as a function of electron density (solid lines). When the plasma density was in the order of 10^{18} cm^{-3}, the theory could well reproduce the experimental energy loss of 4.3-MeV/u ions. As the electron density increases beyond 10^{19} cm^{-3}, the difference between the theory and the experiment increased and reached 15% at the peak density. For 6.0-MeV/u ions, the discrepancy appeared remarkably even at electron densities below 10^{19} cm^{-3}, where the energy losses well agreed with the values calculated for fully stripped ions (broken line). These results indicate that the projectile ions had higher mean charge than the predicted values, particularly for 6.0-MeV/u injection energy. Density effects such as ladderlike excitation and ionization may explain this remarkable increase in the mean charge. The difference in the ionization rate coefficients between 4.3-MeV/u and 6-MeV/u ions, however, was too small to explain the differ-

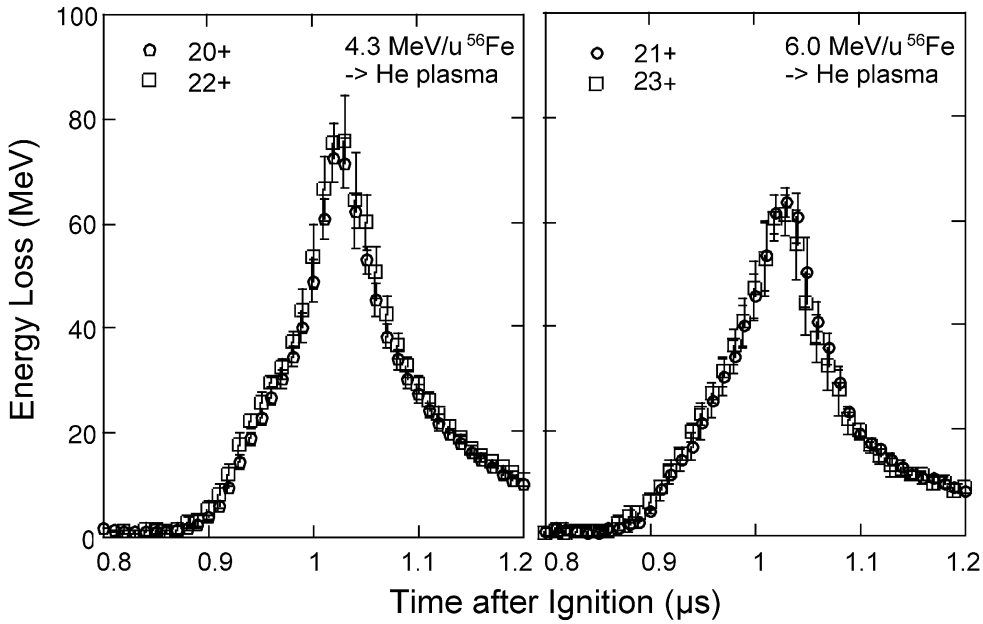

Fig. 3. Time evolution of energy loss of 4.3-MeV/u or 6.0-MeV/u ^{56}Fe in a *z*-pinch helium plasma. Error bars represent standard deviation of shot-to-shot fluctuations.

https://doi.org/10.1017/S0263034602211027 Published online by Cambridge University Press

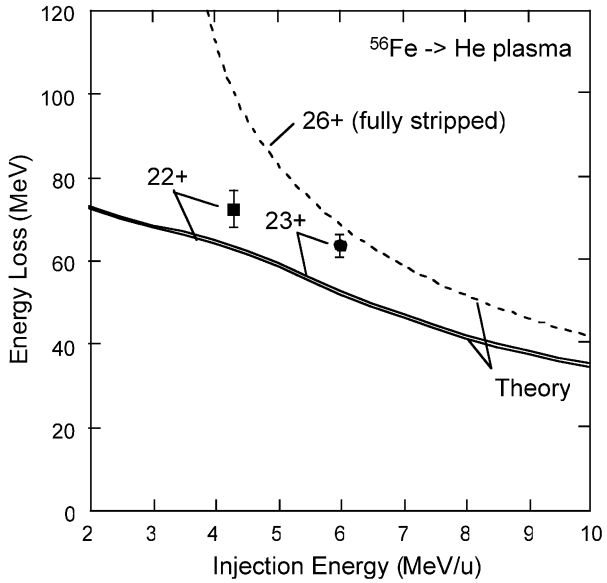

Fig. 4. Dependence of energy losses of 4.3-MeV/u $^{56}Fe^{22+}$ and 6.0-MeV/u $^{56}Fe^{23+}$ on projectile velocity. Solid lines are theoretical curves for $^{56}Fe^{22+}$ (lower) and $^{56}Fe^{23+}$(upper), respectively. A broken line represents a theoretical curve for fully stripped projectiles without charge exchanges in plasma.

ence in the density dependence. Interaction experiments using a proton beam planed in the near future will reveal the projectile effective charge in the plasma target and give us physical insights into this open question.

5. CONCLUSION

We successfully observed the energy loss of 4.3-MeV/u or 6.0-MeV/u ^{56}Fe ions in a dense helium plasma with an electron density above 10^{19} cm^{-3} by optimizing the *z*-pinch-discharge conditions and the beam transport. At relatively low electron density, the observed energy loss of 4.3-MeV/u ions well agreed with the theoretical predictions. We found that the difference between the experiment and the theory became remarkable with increasing electron density or projectile energy, which indicated the acceleration of the ionization processes due to density effects.

ACKNOWLEDGMENT

This work was partially supported by Grant-in-Aid for Encouragement of Young Scientists, Japan Society for the Promotion of Science, No. 13780394.

REFERENCES

Aoki, T., Horioka, K. & Ogawa, M. (1995). Numerical study of coaxial double z-pinch for resonant photopumping x-ray laser. *NIFS-PROC* **23**, 124–135.

Büscher, S., Glenzer, S., Wrubel, Th. & Kunze, H.-J. (1996). Investigation of the He_{II} P_{α} and He_{II} P_{β} *transitions at high densities. J. Phys. B: At. Mol. Opt. Phys.* **29**, 4107–4125.

Couillaud, C., Deicas, R., Nardin, Ph., Beuve, M.A., Beuve, J.M., Guihaume, J.M., Renaud, M., Cukier, M., Deutsch, C. & Maynard, G. (1994). Ionization and stopping of heavy ions in dense laser-ablated plasmas. *Phys. Rev. E* **49**, 1545–1562.

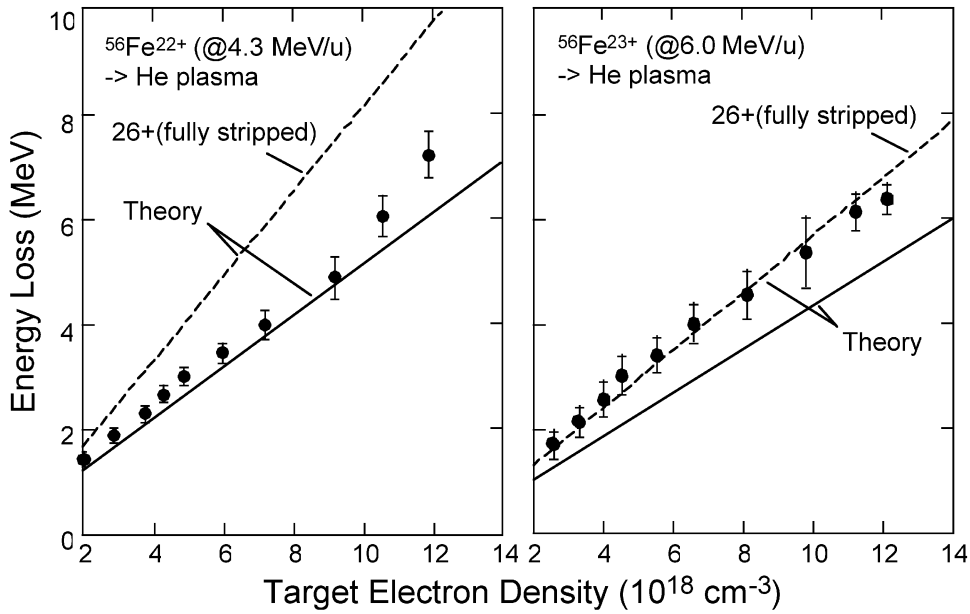

Fig. 5. Dependence of energy loss of 4.3-MeV/u or 6.0-MeV/u ^{56}Fe on plasma electron density. Solid lines are theoretical predictions. Broken lines represent energy loss of fully stripped projectiles without charge exchanges in plasma.

https://doi.org/10.1017/S0263034602211027 Published online by Cambridge University Press

Griem, H.R. (1997). *Principles of Plasma Spectroscopy*. Cambridge: Cambridge University Press.

Hasegawa, J., Nakajima, Y., Sakai, K., Yoshida, M., Fukata, S., Nishigori, K., Kojima, M., Oguri, Y., Nakajima, M., Horioka, K., Ogawa, M., Neuner, U. & Murakami, T. (2001). Energy loss of 6 MeV/u iron ions in partially ionized helium plasma. *Nucl. Instrum. Methods A* **464**, 237–242.

Hoffmann, D.H.H., Weyrich, K., Wahl, H., Gardés, D., Bimbot, R. & Fleurier, C. (1990). Energy loss of heavy ions in a plasma target. *Phys. Rev. A* **42**, 2313–2321.

Jacoby, J., Hoffmann, D.H.H., Laux, W., Müller, R.W., Wahl, H., Weyrich, K., Boggasch, E., Heimrich, B., Stöckl, C., Wetzler, H. & Miyamoto, S. (1995). Stopping of heavy ions in a hydrogen plasma. *Phys. Rev. Lett.* **74**, 1550–1553.

Peter, Th. & Meyer-ter-Vehn, J. (1991). Energy loss of heavy ions in dense plasma. II. Nonequilibrium charge states and stopping powers. *Phys. Rev. A* **43**, 2015–2030.

Young, F.C., Mosher, D., Stepanakis, S.J., Goldstein, S.A. & Mehlhorn, T.A. (1982). Measurements of enhanced stopping of 1-MeV deuterons in target-ablation plasmas. *Phys. Rev. Lett*. **49**, 549–553.

https://doi.org/10.1017/S0263034602211027 Published online by Cambridge University Press